

Mechanism of spironolactone-induced Ca^{2+} increase in rat testicular arteriole smooth muscle cells revealed by real-time laser scanning confocal microscopy

Yasunori Tamagawa¹, Tomoyuki Saino¹, Makoto Matsuura², Makoto Oikawa¹, and Yoh-ichi Satoh¹

Department of ¹Anatomy (Cell Biology), School of Medicine, and ²Advanced Pharmaceutics, School of Pharmacy, Iwate Medical University, Yahaba, Iwate, Japan

Summary. We reported previously that spironolactone (SPL) induced an increase in intracellular Ca^{2+} concentration ($[\text{Ca}^{2+}]_i$) in rat testicular arteriole smooth muscle cells. In the present study, we further investigated the mechanism of SPL-induced $[\text{Ca}^{2+}]_i$ dynamics in rat arteriole smooth muscles. The increase in $[\text{Ca}^{2+}]_i$ induced by SPL (300 μM) was markedly inhibited in extracellular Ca^{2+} -free conditions and in the presence of diltiazem or gadolinium. In contrast, the phospholipase C inhibitor (U73122), did not affect the SPL-induced increase in $[\text{Ca}^{2+}]_i$, similar to what was observed for 2-aminoethoxydiphenyl borate (2-APB: an inhibitor of inositol triphosphate (IP_3)-dependent Ca^{2+} mobilization). Moreover, the protein kinase A (PKA) inhibitor H89 partially inhibited the SPL-induced increase in $[\text{Ca}^{2+}]_i$, whereas the protein kinase C (PKC) inhibitor GF109203X did not. Either suramin (a non-specific G protein antagonist) or NF449 (an inhibitor of the α -subunit of the stimulatory G protein G_{sa}), partially blocked the SPL-induced increase in $[\text{Ca}^{2+}]_i$. Similarly, either mifepristone, a glucocorticoid-receptor antagonist, or flutamide, a non-steroidal antiandrogen drug, partially blocked the SPL-induced increase in $[\text{Ca}^{2+}]_i$. We suggest that the

SPL-induced increase in $[\text{Ca}^{2+}]_i$ in arterioles is mediated both by Ca^{2+} influx from the extracellular fluid and by Ca^{2+} mobilization from internal Ca^{2+} stores, with the former being dominant. We thus propose that SPL interacts with both extracellular (i.e., G-protein-coupled-type) and intracellular (e.g., glucocorticoid) receptors in rat testicular arterioles, which is followed by an increase in intracellular Ca^{2+} that causes smooth-muscle contraction.

Introduction

Spironolactone (SPL) is a mineralocorticoid receptor antagonist that can reverse cardiac fibrosis in both the ventricles (Brilla *et al.*, 1993). SPL predominantly acts as a competitive antagonist of the aldosterone (or mineralocorticoid) receptor and belongs to a class of pharmaceutical drugs known as potassium-sparing diuretics. In addition to several previously reported clinical studies, recent reports have shown blood pressure-independent beneficial effects of mineralocorticoid-receptor blockers against renal injury in several animal models of hypertension. In stroke-prone spontaneously hypertensive rats, SPL decreased proteinuria and histological renal/vascular damage and increased survival in the absence of blood pressure effects (Rocha *et al.*, 1998). A study performed in rats showed that SPL prevents collagen proliferation in the myocardium after infarction, which complements previous findings (Mill *et al.*, 2003).

It is well known that the dynamics of intracellular Ca^{2+} concentration ($[\text{Ca}^{2+}]_i$) play a fundamental role in the

Received November 21, 2012

Address for correspondence: Dr. Tomoyuki Saino, Department of Anatomy, School of Medicine, Iwate Medical University, 2-1-1 Nishitokuda, Yahaba, Iwate 028-3694, Japan
Tel: +81-19-651-5111, Fax: +81-19-908-8006
E-mail: tsaino@iwate-med.ac.jp

regulation of various cellular functions (Bootman *et al.*, 2001), including the contraction of smooth muscles (van Breemen and Saida, 1989; Somlyo and Somlyo, 1994; Saino *et al.*, 2002; Berridge, 2008). We previously reported that SPL-induced increase in $[Ca^{2+}]_i$ can be caused both by a Ca^{2+} influx from the extracellular fluid and by Ca^{2+} mobilization from internal Ca^{2+} stores, with the former being dominant (Tamagawa *et al.*, 2009). In addition, SPL is a synthetic steroidal antimineralocorticoid agent with additional antiandrogen, weak progestogen, and as some indirect estrogen and glucocorticoid properties. Steroid-hormone receptors are generally intracellular receptors (typically cytoplasmic) and initiate signal transduction for steroid hormones, which leads to changes in gene expression over a time period of hours to days.

Thus, the aim of the present study was to clarify the effects of SPL on arterioles more clearly than before. We initially predicted that SPL would only interact with intracellular receptors. Our results, however, lead us to suggest that SPL interacts with both extracellular and intracellular receptors, which induces an increase in $[Ca^{2+}]_i$ and leads to smooth-muscle contraction in rat testicular arterioles.

Materials and Methods

Preparation of arterioles

Experiments were conducted according to the guidelines of the ethics committee for animal treatment of Iwate Medical University. Under anesthesia with carbon dioxide gas, adult male rats (Wistar; age, 8–12 weeks; body weight, 250–400 g) were perfused via the left cardiac ventricle using Ringer's solution (147 mM NaCl, 4 mM KCl, and 2.25 mM $CaCl_2$) at room temperature (20–25°C). After washing out the blood from the vessels, the testes were removed and placed in Hepes-buffered Ringer's solution (HR); 118 mM NaCl, 4.7 mM KCl, 1.25 mM $CaCl_2$, 1.13 mM $MgCl_2$, 1 mM NaH_2PO_4 , 5.5 mM D-glucose, MEM amino acids solution (Gibco, Grand Island, NY, USA), 0.2% bovine serum albumin (Sigma, St. Louis, MO, USA), and 10 mM Hepes, adjusted with NaOH to pH 7.4). Arterial trees were then isolated from testes and the connective tissues surrounding vessels were carefully removed using fine forceps. The specimens were subsequently incubated in HR containing purified collagenase (100 U/ml; Elastin Products, Owensville, MO, USA) for 2 h at room temperature.

Scanning electron microscopy (SEM)

The isolated arterioles were fixed in 0.25% glutaraldehyde

(Nacalai Tesque, Kyoto, Japan) and 4% paraformaldehyde (Merck KGaA, Darmstadt, Germany) in phosphate-buffered saline (0.1 M) for ~2 days at 4°C. The arterioles were then digested with KOH, followed by incubation with crude type II collagenase (Worthington, Lakewood, NJ, USA) (Ushiwata and Ushiki, 1990). The cells were postfixed with 1% osmium tetroxide for 1 h, dehydrated in a graded series of ethanol solutions, critical point dried, coated with platinum in an ion sputtering coater (E-1030; Hitachi Co, Hitachi, Japan) and observed under a scanning electron microscope (S-2300; Hitachi Co.).

Intracellular Ca^{2+} imaging

Isolated live arteriole specimens were placed on a glass cover slip, set in a perfusion chamber, and incubated with 10 μ M Indo-1/AM (a Ca^{2+} -sensitive fluorescent dye; Dojindo, Kumamoto, Japan) in HR solution for 1 h at 37°C. Indo-1 is a ratiometric dye for the quantitative determination of $[Ca^{2+}]_i$. The emission maximum of Indo-1 shifted from 475 nm in Ca^{2+} -free medium to 400 nm when the dye solution was saturated with Ca^{2+} . The ratio of an emission intensity shorter than 440 nm to one longer than 440 nm was used to estimate $[Ca^{2+}]_i$; a greater ratio indicated higher $[Ca^{2+}]_i$. Artifacts, including photobleaching and/or dye leakage, can be eliminated using this ratiometry. Time course of $[Ca^{2+}]_i$ dynamics in restricted areas (region of interest; ROI) was measured using temporal analyses. The size of the ROIs was approximately 3 μ m².

We used a real-time confocal laser scanning microscope (RCM/Ab; a modified version of the Nikon model RCM-8000 microscope; Nikon, Tokyo, Japan) to measure the dynamics of $[Ca^{2+}]_i$. Cells loaded with Indo-1 were exposed to an ultraviolet-beam (351 nm). An argon-ion laser was equipped with an inverted microscope (TE-300; Nikon), and the fluorescence was passed through a water-immersion objective lens (Nikon C Apo 40 \times ; N.A., 1.15) to a pinhole diaphragm. To decrease the electrical noise and reduce photodamage, each image was integrated from 8 frames and sequential images were intermittently acquired every 1 sec, although the shortest acquisition time per image was 1/15 sec using this system. The digital images from the laser scanning microscopic imaging were composed of 512 \times 480 pixels with a density resolution of 8 bits/pixel. The intensity of fluorescence displayed 256 pseudo colors, with red representing high $[Ca^{2+}]_i$ and purple and blue representing low $[Ca^{2+}]_i$.

Three-dimensionally reconstructed fluorescent images were acquired consecutively using a high-speed laser scanning microscope (CSUX-1; Yokogawa Electric Corporation, Tokyo, Japan) equipped with an EMCCD

camera (iXon3; Andor Technology, Belfast, UK). Arterioles were loaded with Calcein-AM (5 μM ; a cell-permeant fluorescent dye; Dojindo) in HR solution for 1 h at 37°C and were then exposed to a diode laser (488 nm) (Vortran Laser Technology, Sacramento, USA).

Perfusion

The $[\text{Ca}^{2+}]_i$ dynamics of arterioles was observed in a perfusion chamber as quickly as possible after the loading of the dye. After perfusion with standard HR for a few minutes, intact arterioles showing completely sufficient fluorescent signals were selected. Injured cells in the arterioles, which exhibited high $[\text{Ca}^{2+}]_i$ at resting conditions, were excluded from the subsequent temporal analyses.

After a brief rinse in HR solution, the specimens were continuously perfused with HR containing the following drugs or modulators: SPL (300 μM ; Wako, Japan), thapsigargin (a microsomal Ca^{2+} -ATPase inhibitor, 2 μM ; Sigma), GdCl_3 (a nonspecific cation-channel blocker, 100 μM ; Wako), diltiazem (an L-type Ca^{2+} channel blocker, 50 μM ; Sigma), U73122 (a specific inhibitor of phospholipase C (PLC), 5 μM ; Sigma), SQ22536 (an adenylyl cyclase inhibitor, 100 μM ; Sigma), 2-aminoethoxydiphenyl borate (2-APB: an antagonist of the inositol triphosphate (IP_3) receptor, 100 μM ; Tocris, Bristol, UK), GF109203X (an inhibitor of protein kinase C (PKC), 2 μM ; Enzo Life Sciences, Ann Arbor, USA), H89 (an inhibitor of protein kinase A (PKA), 100 μM ;

Enzo Life Sciences), suramin (a non-specific G protein antagonist, 90 μM ; Research Biochemicals International, Natick, MA), NF449 (a selective antagonist of the α -subunit of the stimulatory G protein (G_{sa}), 30 μM ; Tocris), $\text{PKI}_{(14-22)}$ (an inhibitor of PKA, 2 μM ; Enzo Life Sciences), pertussis toxin (an inhibitor of G_i subunits, 100 ng/ml; Sigma), propranolol (an inhibitor of the β receptor of catecholamines, 20 μM ; Sigma), flutamide (a androgen-receptor antagonist, 10 μM ; Sigma), mifepristone (a progesterone- and glucocorticoid-receptor antagonist, 50 μM ; Tocris), ICI 182,780 (an estrogen-receptor antagonist, 2 μM ; Santa Cruz Biotechnology, Santa Cruz, USA), G15 (a membrane estrogen-receptor antagonist, 10 μM ; Tocris), and aldosterone (a corticosteroid hormone, 1 μM ; Sigma). Ca^{2+} -deficient solutions were prepared by replacing CaCl_2 with EGTA (1.0 mM; Sigma). Doses of SPL and others used in the present study were determined by preliminary studies.

Results

Structure of arteriole specimens

Figure 1 shows images of arterioles obtained using SEM and real-time confocal laser scanning microscopy. Arterioles were characterized by the presence of spindle-shaped smooth muscle cells running in a circular fashion. There was little morphological deterioration after the isolation procedures. Confocal laser scanning microscopy

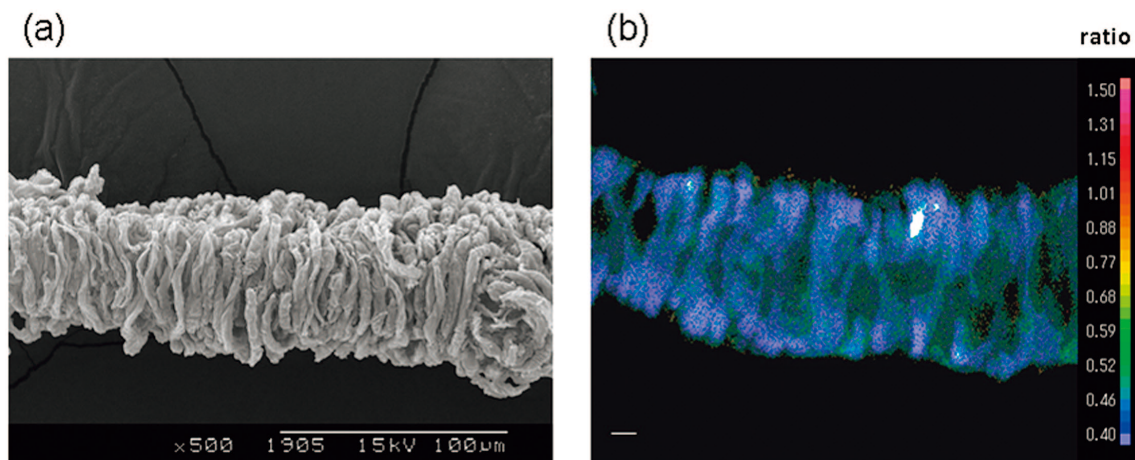


Fig. 1. Arteriole specimens from testicular tissues used in the present study. **a:** Scanning electron micrograph. Bar: 100 μm . **b:** Confocal fluorescent image showing the pseudocolor of indo-1 ratio. Smooth muscles are shown as spindle-shaped profiles and maintained a circular arrangement. Damaged cells with a high $[\text{Ca}^{2+}]_i$ level were rare, which ensured the functional integrity of the specimen. Bar: 10 μm , Color scale bar, the fluorescence ratio represents $[\text{Ca}^{2+}]_i$.

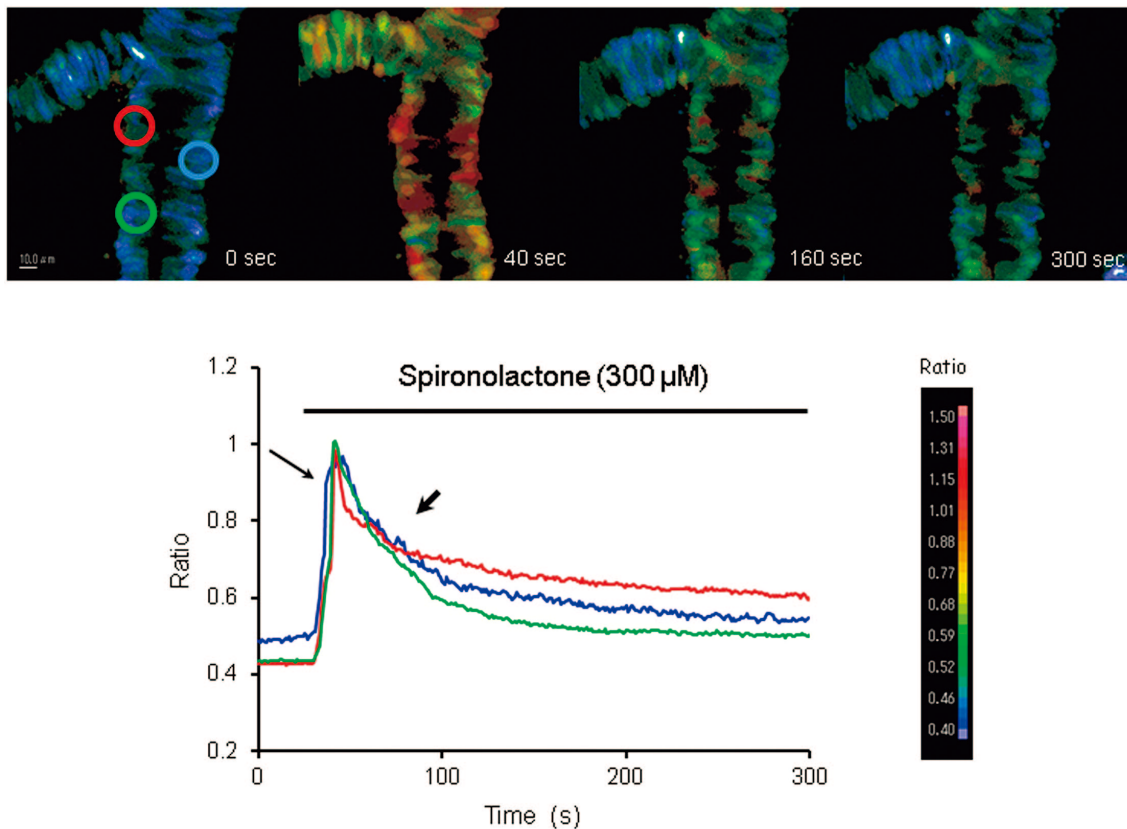


Fig. 2. Pseudocolor images and time course analysis of SPL-induced $[Ca^{2+}]_i$ dynamics. The temporal changes of $[Ca^{2+}]_i$ in the 3 ROIs are depicted (blue, green, and red lines). Note the biphasic $[Ca^{2+}]_i$ dynamics: an initial acute increase (thin arrow) was followed by a gradual decline with oscillatory fluctuations (small thick arrow). Three ROIs were set for these analyses.

also provided clear images of smooth-muscle profiles. Ratiometric studies showed that the $[Ca^{2+}]_i$ in the unstimulated arterioles was stable and that their ratio was about 0.5 in the absence of agonists.

Effect of SPL on $[Ca^{2+}]_i$ dynamics

Arteriole specimens were perfused with normal HR solution for 5 min before the administration of SPL. During the unstimulated resting period, no spontaneous $[Ca^{2+}]_i$ dynamics was observed in smooth muscles.

The addition of SPL (300 μ M) caused transient $[Ca^{2+}]_i$ dynamics. The response of $[Ca^{2+}]_i$ was biphasic: there was an initial rapid increase in $[Ca^{2+}]_i$, followed by a second gradual decline phase with fine oscillatory fluctuation (number of experiments; $n=18$; Fig. 2). The possibility of the transient contraction of vessels in certain tissues must be considered. During the increase in $[Ca^{2+}]_i$, smooth-

muscle contraction was evident, as assessed using time-lapse three-dimensional reconstruction of arteriole images; in addition, the external diameter decreased by approximately 20%. When the external diameter was compared with the internal caliber of arterioles before (Start) and after (5 sec) the administration of SPL. The two parameters were reduced from 96% to 71% (Fig. 3 ■), from 92% to 57% (Fig. 3 ▲), and from 93% to 76% (Fig. 3 ●), respectively.

Mechanism of SPL-induced $[Ca^{2+}]_i$ dynamics

Two major mechanisms are introduced for increasing $[Ca^{2+}]_i$: (1) Ca^{2+} influx via an ion channel located on the plasma cell membrane and (2) Ca^{2+} mobilization from internal Ca^{2+} stores (e.g., sarcoendoplasmic reticulum) (Berridge *et al.*, 2003). Thus the correlation of the Ca^{2+} influx with the SPL-induced increase in $[Ca^{2+}]_i$ was

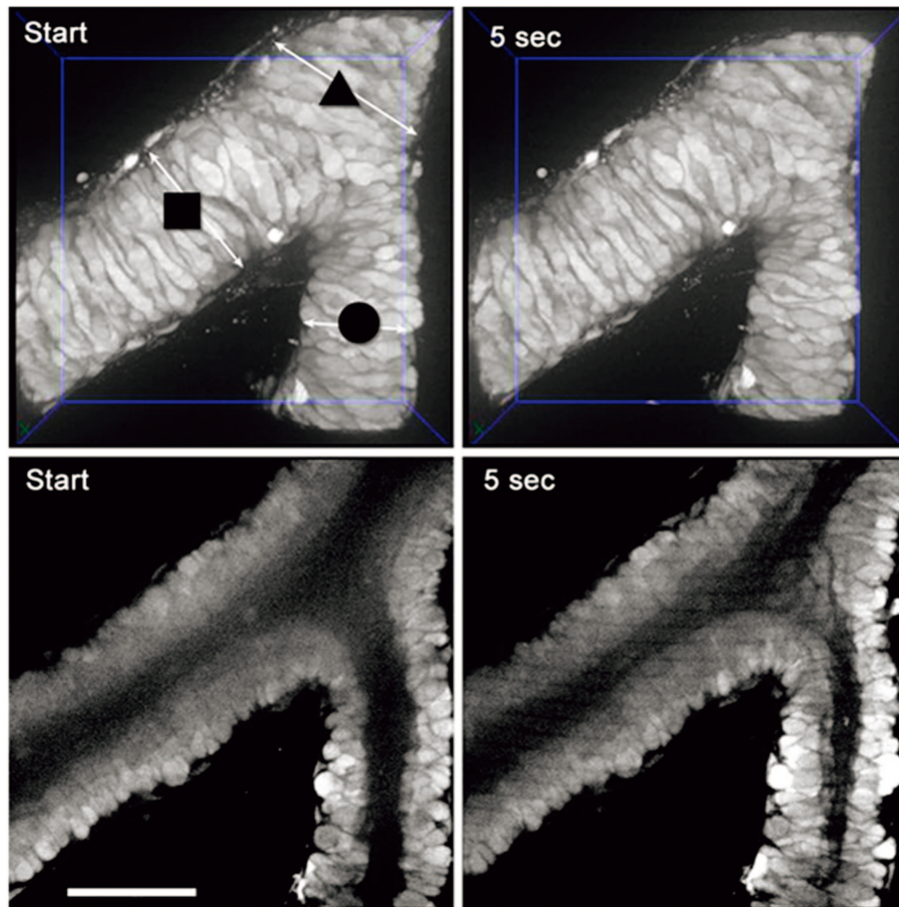


Fig. 3. Three-dimensionally reconstructed fluorescent images of testicular arterioles. Arterioles were loaded with Calcein-AM ($5 \mu\text{M}$). The external diameter and internal caliber of the arteriole were compared, before (Start) and after (5 sec) the administration of SPL. The external diameter and the internal caliber reduced from 96% to 71% (■), from 92% to 57% (▲), and from 93% to 76% (●), respectively.

observed under extracellular Ca^{2+} -free conditions ($n=14$; Fig. 4a) in the presence of either diltiazem ($50 \mu\text{M}$, $n=14$; Fig. 4b) or GdCl_3 ($100 \mu\text{M}$, $n=12$; data not shown). The inhibition of Ca^{2+} influx under these conditions led to a considerable suppression of the initial increase in $[\text{Ca}^{2+}]_i$, and to the disappearance of the slow-decline phase (Fig. 4a, b). These data indicate that Ca^{2+} influx plays a pivotal role either in the initial increase or in the decline phase of SPL-induced $[\text{Ca}^{2+}]_i$ dynamics.

Thapsigargin was then used ($n=10$) to investigate the possible contribution of Ca^{2+} mobilization from internal stores. The depletion of Ca^{2+} stores by thapsigargin ($2 \mu\text{M}$) inhibited the initial increase in $[\text{Ca}^{2+}]_i$ considerably, indicating that Ca^{2+} mobilization correlates with the initial

phase of SPL-induced $[\text{Ca}^{2+}]_i$ dynamics (Fig. 4c). Thapsigargin had few effects on the decline phase of SPL-induced $[\text{Ca}^{2+}]_i$ dynamics, indicating that the replenishment of Ca^{2+} from the external environment without Ca^{2+} mobilization, is essential in the decline phase.

Generally, metabotropic receptors are G-protein linked, and the stimulation of G proteins activates PLC, which cleaves membrane-bound phosphatidylinositol biphosphate to generate IP_3 , and diacylglycerol. IP_3 subsequently causes Ca^{2+} mobilization from internal stores (Berridge, 2009). To determine if this mechanism of Ca^{2+} mobilization was involved in the SPL-dependent increase in $[\text{Ca}^{2+}]_i$, the effect of U73122 was assayed. U73122 ($5 \mu\text{M}$) did not inhibit the SPL-induced increase in $[\text{Ca}^{2+}]_i$ ($n=12$;

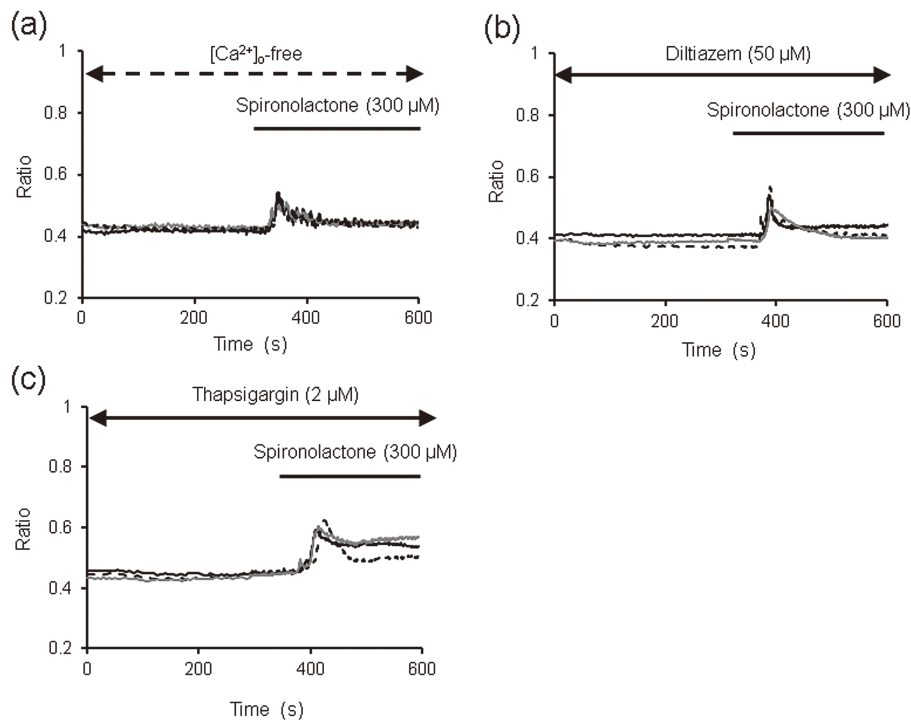


Fig. 4. Time-course analyses of the SPL-induced $[Ca^{2+}]_i$ dynamics under various modulations. The temporal changes of $[Ca^{2+}]_i$ in the 3 ROIs are depicted (black, gray, and dotted lines). **a:** SPL-induced $[Ca^{2+}]_i$ dynamics under extracellular Ca^{2+} -free conditions ($[Ca^{2+}]_o$ -free). **b:** SPL-induced $[Ca^{2+}]_i$ dynamics in the presence of diltiazem ($50 \mu M$). **c:** SPL-induced $[Ca^{2+}]_i$ dynamics after depleting intracellular Ca^{2+} stores via treatment with thapsigargin ($2 \mu M$). Three ROIs were set for these analyses.

Fig. 5a). In addition, 2-APB ($100 \mu M$) did not block this increase completely ($n=8$; Fig. 5b).

Next, we attempted to clarify whether the receptors of SPL interact with membrane receptors (e.g., G proteins) using agonists/antagonists of G proteins. The pertussis toxin catalyzes the ADP ribosylation of the α_i subunit of heterotrimeric G proteins. This prevents these G proteins from interacting with G-protein-coupled receptors (GPCRs) located on the cell membrane, thus interfering with intracellular communication (Burns 1988). Perfusion with pertussis toxin (100 ng/ml) activated the SPL-induced $[Ca^{2+}]_i$ dynamics slightly ($n=9$; Fig. 6a). NF449 reduces the association rate of guanosine 5'-[γ -thio] triphosphate binding to G_{sa} and inhibits the stimulation of adenylyl cyclase activity in S49 cyc-membranes. NF449 ($30 \mu M$) is partially blocked the SPL-dependent increase in $[Ca^{2+}]_i$ ($n=8$; Fig. 6b). Suramin inhibits the activation of heterotrimeric G proteins in a variety of other GPCRs with varying potency and has been used in research as a

broad-spectrum antagonist of P2 receptors. Here, suramin ($50 \mu M$) also partially blocked the SPL-dependent increase in $[Ca^{2+}]_i$ ($n=10$; Fig. 6c). These findings suggest that SPL interacts with GPCRs.

To determine whether protein kinases are involved in the SPL-dependent increase in $[Ca^{2+}]_i$, the effects of several kinase antagonists were assayed. H89 ($100 \mu M$) partially inhibited the SPL-induced increase in $[Ca^{2+}]_i$ ($n=9$; Fig. 7a). Moreover, $PKI_{(14-22)}$ ($2 \mu M$) had a similar effect ($n=8$; data not shown). SQ22536 ($100 \mu M$) also did not completely block this increase ($n=10$; Fig. 7b). Arterioles were also incubated with the PKC inhibitor GF109203X ($2 \mu M$) for 5 min before the addition of SPL, but this inhibitor had no effect on SPL-induced increase in $[Ca^{2+}]_i$ ($n=8$; data not shown). Propranolol is a sympatholytic non-selective β blocker. In addition, the β adrenergic receptors are a class of metabotropic GPCRs that are linked to G_s proteins. The SPL-induced increase in $[Ca^{2+}]_i$ was not inhibited in the presence of propranolol

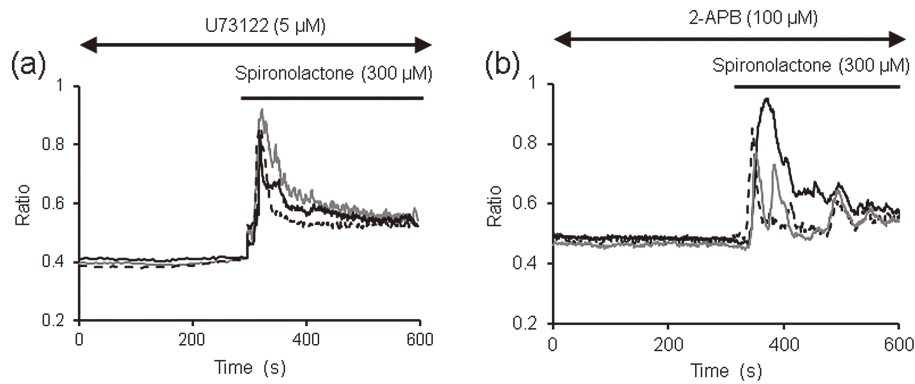


Fig. 5. A role for the mobilization of Ca^{2+} from intracellular Ca^{2+} stores in SPL-induced $[\text{Ca}^{2+}]_i$ changes. SPL (300 μM) induced an increase in $[\text{Ca}^{2+}]_i$ in cells after blocking phospholipase C by treatment with U73122 (5 μM) (a). Treatment with the IP_3 -receptor antagonist 2-APB (100 μM) also failed to inhibit SPL-induced increase in $[\text{Ca}^{2+}]_i$ (b). Three ROIs were set for these analyses.

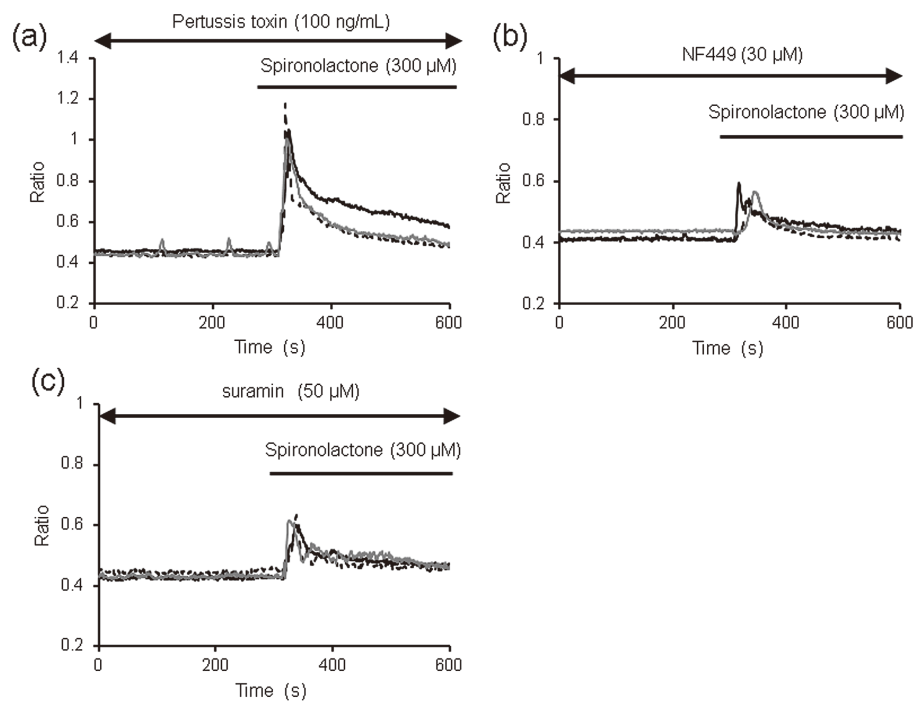


Fig. 6. A role for G-protein-coupled membrane receptors in SPL-induced $[\text{Ca}^{2+}]_i$ changes. Time-course analyses of the SPL-induced $[\text{Ca}^{2+}]_i$ dynamics under treatment with blockers of G proteins. **a:** Effect of the pertussis toxin (100 ng/ml). **b:** Effect of NF449 (30 μM). **c:** Effect of suramin (50 μM). Time-course analyses of the SPL-induced $[\text{Ca}^{2+}]_i$ dynamics under various modulations. The temporal changes of $[\text{Ca}^{2+}]_i$ for three ROIs are depicted (black, gray, and dotted lines). Three ROIs were set for these analyses.

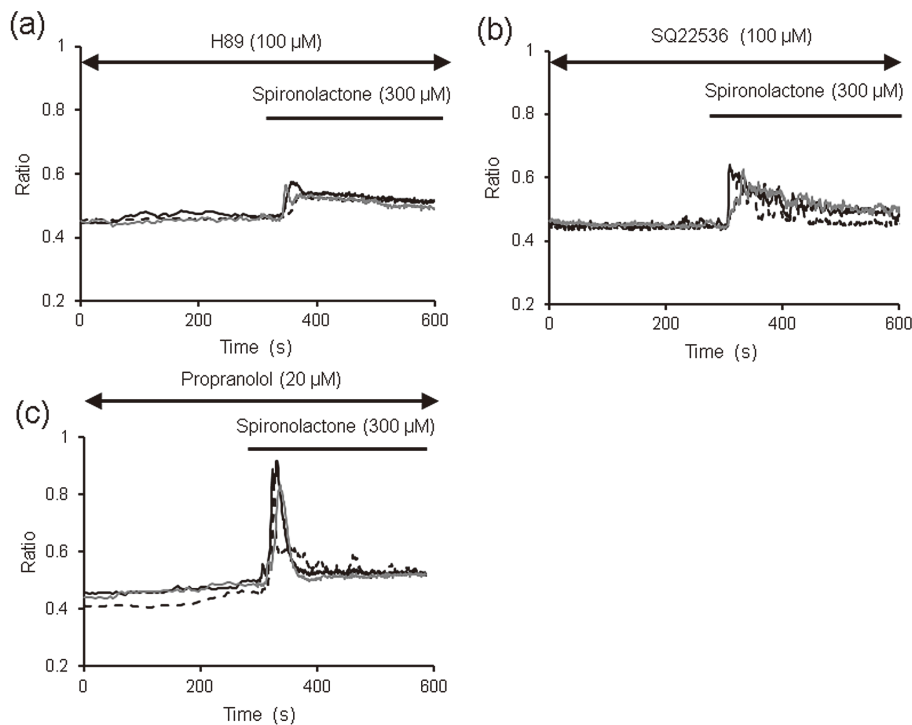


Fig. 7. Time-course analyses of the SPL-induced $[Ca^{2+}]_i$ dynamics under treatment with blockers of PKA, an adenylyl cyclase, and a β blocker. **a:** Effect of H89 (100 μ M). **b:** Effect of SQ22536 (100 μ M). **c:** Effect of propranolol (20 μ M). Time-course analyses of the SPL-induced $[Ca^{2+}]_i$ dynamics under various modulations. The temporal changes of $[Ca^{2+}]_i$ in 3 ROIs are depicted (black, gray, and dotted lines). Three ROIs were set for these analyses.

(20 μ M) ($n=8$; Fig. 7c), indicating that SPL does not stimulate catecholaminergic β receptors. These findings confirm the view that cAMP pathways (especially the PKA pathway) partially contribute to SPL-mediated $[Ca^{2+}]_i$ increase in testicular arterioles.

We further attempted to determine whether the receptors of SPL interact with intracellular receptors. Because SPL is an agonist of aldosterone which affects the transport of Na^+ , K^+ , and Cl^- in kidney epithelial cells, we examined whether aldosterone was involved in the SPL-induced dynamics between $[Ca^{2+}]_i$ and smooth muscles. Aldosterone (1 μ M) did not inhibit the SPL-induced increase in $[Ca^{2+}]_i$ ($n=7$; Fig. 8a). In the case of SPL-induced Ca^{2+} dynamics, there was no relationship between SPL and aldosterone. To determine the involvement of the glucocorticoid receptor or the androgen receptor in the SPL-dependent increase in $[Ca^{2+}]_i$, the effect of several antagonists of these receptors were assayed. ICI 182,780 (2 μ M) failed to inhibit the increase in Ca^{2+} in testicular arteriole smooth muscle cells ($n=8$; Fig. 8b). In

the presence of G15 (a selective antagonist of GPR30, a non-nuclear estrogen receptor; 10 μ M), stimulation by SPL also failed to inhibit an increase in $[Ca^{2+}]_i$ ($n=8$; data not shown). Mifepristone is a progesterone-receptor antagonist and a powerful glucocorticoid-receptor antagonist that has occasionally been used to treat refractory Cushing's syndrome. The SPL-induced increase in $[Ca^{2+}]_i$ was partially inhibited in the presence of mifepristone (50 μ M) ($n=10$; Fig. 8c). Flutamide is a nonsteroidal antiandrogen drug that is primarily used to treat prostate cancer. It competes with testosterone and its powerful metabolite, dihydrotestosterone (DHT) for binding to androgen receptors in the prostate gland. Flutamide also partially blocked the SPL-induced increase in $[Ca^{2+}]_i$ ($n=9$; Fig. 8d).

Discussion

Ca^{2+} responses have been examined mainly in cultured or isolated vascular smooth-muscle cells using various

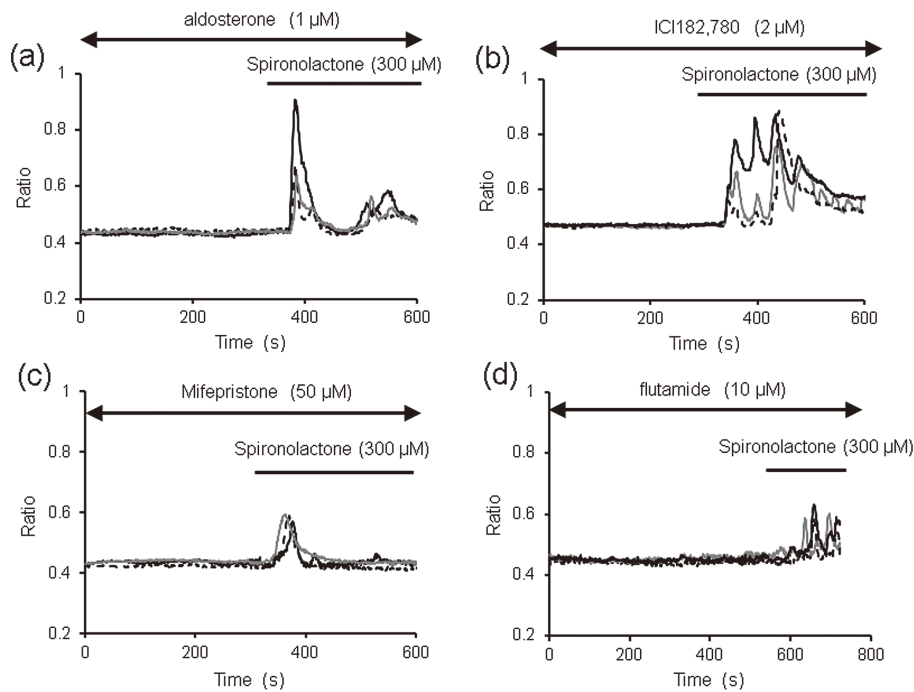


Fig. 8. A role for mineralocorticoid, glucocorticoid, estrogen, and androgen receptors in SPL-induced $[\text{Ca}^{2+}]_i$ changes. Time-course analyses of the SPL-induced $[\text{Ca}^{2+}]_i$ dynamics in cells. **a:** Effect of aldosterone ($1 \mu\text{M}$). **b:** Effect of ICI 182,780 ($2 \mu\text{M}$). **c:** Effect of mifepristone ($50 \mu\text{M}$). **d:** Effect of flutamide ($10 \mu\text{M}$). Time-course analyses of for the SPL-induced $[\text{Ca}^{2+}]_i$ dynamics under various modulations. The temporal changes of $[\text{Ca}^{2+}]_i$ in 3 ROIs are depicted (black, gray, and dotted lines). Three ROIs were set for these analyses.

imaging techniques (Iino *et al.*, 1994; Yip and Marsh, 1996; Li *et al.*, 1997; Bolton and Gordienko, 1998; Jaggar *et al.*, 1998). In the course of the culture of vascular smooth-muscle cells, the functional coupling between the sarcoendoplasmic reticulum and mitochondria was altered during the dedifferentiation and/or redifferentiation process, which occurs in rat aortic smooth-muscle cells in culture (Vallot *et al.*, 2001). It is also possible that the characteristics of the smooth-muscle cells of intact arterioles are different from those of cultured cells. In this context, it is crucial to analyze intact smooth-muscle cells.

In the present study, SPL led to an increase in $[\text{Ca}^{2+}]_i$ in the smooth muscles of arterioles. Based on the present data, we concluded that the initial increase of the SPL-induced dynamics of $[\text{Ca}^{2+}]_i$ was caused by Ca^{2+} influx and Ca^{2+} mobilization and that the subsequent decline phase (with fine oscillatory fluctuations) was correlated with Ca^{2+} influx.

In general, changes in $[\text{Ca}^{2+}]_i$ after GPCR activation are

thought to be due to IP_3 -mediated Ca^{2+} mobilization from an internal store, such as the sarcoendoplasmic reticulum (Berridge, 2009). SPL-mediated $[\text{Ca}^{2+}]_i$ changes were not inhibited by 2-APB (which antagonizes the calcium-releasing action of IP_3) and U73122, suggesting that testicular arterioles possess IP_3 -independent as well as IP_3 -dependent Ca^{2+} mobilization systems.

Various steroids can elicit vascular contraction (Gros *et al.*, 2007) and activation of a plasma-membrane receptor of aldosterone induces the IP_3 -mediated dynamics of $[\text{Ca}^{2+}]_i$ (Wehling, 2005). A novel estrogen receptor, GPR30, which belongs to the family of seven-transmembrane GPCRs, exhibits various rapid biological responses to estrogen (Prossnitz *et al.*, 2008). GPR30 has recently been shown to be expressed in the vascular system (Broughton *et al.*, 2010; Meyer *et al.*, 2011). Therefore, the present study was performed on the hypothesis that the effects of SPL on cognitive performance are mediated by GPCRs. The experiments using the pertussis toxin, NF449, and suramin actually revealed the existence of a

relationship between SPL and GPCRs, with the exception of β receptors. Moreover, the dependence of SPL-induced Ca^{2+} increase on PKA (which was observed in the presence of H89, PKI, and SQ22536) was an important finding of the present study.

SPL has the same steroid nucleus, and transiently activates membrane receptors and interacts with some intracellular receptors. Because of the antiandrogen effects that result from these actions, SPL is frequently used to treat a variety of cosmetic conditions in which androgen hormones (such as testosterone and DHT) play a role (Hughes and Cunliffe, 1988). In addition, SPL inhibits steroid 11β -hydroxylase; notably, this enzyme is essential for the production of the glucocorticoid hormones cortisol and hydrocortisone. Hence, in theory, glucocorticoids would be lowered by SPL, in addition to mineralocorticoids. The results of our experiments suggest that SPL interacts with glucocorticoid and androgen receptors. The mechanism mentioned above is consistent with our data.

Taking every factor into consideration, the effect of SPL in arteriole smooth-muscle cells appears to occur via both extracellular (e.g., a G-protein-coupled type, especially adenylyl cyclase) and intracellular (i.e., glucocorticoid and androgen) receptors, which leads to an increase in intracellular Ca^{2+} and causes smooth-muscle contraction in rat testicular arterioles.

Grant Support

This work was supported by research grants from the Ministry of Education, Culture and Science of Japan (T.S.; 24590259) and from the Promotion and Mutual Aid Corporation for Private Schools of Japan. Part of this work was performed at the Advanced Medical Science Center of Iwate Medical University, which also provided financial support.

References

- Berridge MJ: Smooth muscle cell calcium activation mechanisms. *J Physiol* 586: 5047–5061 (2008).
- Berridge MJ: Inositol trisphosphate and calcium signalling mechanisms. *Biochim Biophys Acta* 1793: 933–940 (2009).
- Berridge MJ, Bootman MD, Roderick HL: Calcium signalling: dynamics, homeostasis and remodelling. *Nat Rev Mol Cell Biol* 4: 517–529 (2003).
- Bolton TB, Gordienko DV: Confocal imaging of calcium release events in single smooth muscle cells. *Acta Physiol Scand* 164: 567–575 (1998).
- Bootman MD, Lipp P, Berridge MJ: The organisation and functions of local Ca^{2+} signals. *J Cell Sci* 114: 2213–2222 (2001).
- Brilla CG, Matsubara LS, Weber KT: Antifibrotic effects of spironolactone in preventing myocardial fibrosis in systemic arterial hypertension. *Am J Cardiol* 71: 12A–16A (1993).
- Broughton BR, Miller AA, Sobey CG: Endothelium-dependent relaxation by G protein-coupled receptor 30 agonists in rat carotid arteries. *Am J Physiol Heart Circ Physiol* 298: H1055–H1061 (2010).
- Burns DL: Subunit structure and enzymic activity of pertussis toxin. *Microbiol Sci* 5: 285–287 (1988).
- Gros R, Ding Q, Armstrong S, O’Neil C, Pickering JG, Feldman RD: Rapid effects of aldosterone on clonal human vascular smooth muscle cells. *Am J Physiol Cell Physiol* 292: C788–C794 (2007).
- Hughes BR, Cunliffe WJ: Tolerance of spironolactone. *Br J Dermatol* 118: 687–691 (1988).
- Iino M, Kasai H, Yamazawa T: Visualization of neural control of intracellular Ca^{2+} concentration in single vascular smooth muscle cells in situ. *EMBO J* 13: 5026–5031 (1994).
- Jaggard JH, Stevenson AS, Nelson MT: Voltage dependence of Ca^{2+} sparks in intact cerebral arteries. *Am J Physiol* 274: C1755–C1761 (1998).
- Li Z, Zhang Q, Zhao S, Wei M, Shenghui Z, Cong H, Ouda H, Odajima K, Takemura H: Responsiveness of cytosolic free calcium concentration in cultured rat pulmonary arterial smooth muscle cells: confocal microscopic measurement. *Res Commun Mol Pathol Pharmacol* 97: 47–52 (1997).
- Meyer MR, Prossnitz ER, Barton M: The G protein-coupled estrogen receptor GPER/GPR30 as a regulator of cardiovascular function. *Vascul Pharmacol* 55: 17–25 (2011).
- Mill JG, Milanez Mda C, de Resende MM, Gomes Mda G, Leite CM: Spironolactone prevents cardiac collagen proliferation after myocardial infarction in rats. *Clin Exp Pharmacol Physiol* 30: 739–744 (2003).
- Prossnitz ER, Sklar LA, Oprea TI, Arterburn JB: GPR30: a novel therapeutic target in estrogen-related disease. *Trends Pharmacol Sci* 29: 116–123 (2008).
- Rocha R, Chander PN, Khanna K, Zuckerman A, Stier CT Jr.: Mineralocorticoid blockade reduces vascular injury in stroke-prone hypertensive rats. *Hypertension* 31: 451–458 (1998).
- Saino T, Matsuura M, Satoh Y: Application of real-time confocal microscopy to intracellular calcium ion dynamics in rat arterioles. *Histochem Cell Biol* 117: 295–305 (2002).
- Somlyo AP, Somlyo AV: Signal transduction and regulation in smooth muscle. *Nature* 372: 231–236 (1994).

- Tamagawa Y, Saino T, Matsuura M, Satoh Y: The effects of diuretics on intracellular Ca^{2+} dynamics of arteriole smooth muscles as revealed by laser confocal microscopy. *Acta Histochem Cytochem* 42: 121–128 (2009).
- Ushiwata I, Ushiki T: Cytoarchitecture of the smooth muscles and pericytes of rat cerebral blood vessels. A scanning electron microscopic study. *J Neurosurg* 73: 82–90 (1990).
- Vallot O, Combettes L, Lompre AM: Functional coupling between the caffeine/ryanodine-sensitive Ca^{2+} store and mitochondria in rat aortic smooth muscle cells. *Biochem J* 357: 363–371 (2001).
- van Breemen C, Saida K: Cellular mechanisms regulating $[\text{Ca}^{2+}]_i$ smooth muscle. *Annu Rev Physiol* 51: 315–329 (1989).
- Wehling M: Effects of aldosterone and mineralocorticoid receptor blockade on intracellular electrolytes. *Heart Fail Rev* 10: 39–46 (2005).
- Yip KP, Marsh DJ: $[\text{Ca}^{2+}]_i$ in rat afferent arteriole during constriction measured with confocal fluorescence microscopy. *Am J Physiol* 271: F1004–F1011 (1996).